

A Group Theoretical Paradigm for describing the Skeletal Molecular Orbitals of Cluster Compounds. Part 2.† Bispherical Clusters

Roy L. Johnston and D. Michael P. Mingos*

Inorganic Chemistry Laboratory, University of Oxford, South Parks Road, Oxford OX1 3QR

Stone's Tensor Surface Harmonic Theory has been extended to capped and raft clusters where the cluster atoms lie on the surface of two concentric spheres. The skeletal molecular orbitals of these bispherical clusters possess radial as well as tangential nodes. Group theoretical techniques enable the symmetries and quantum numbers L of the skeletal molecular orbitals to be evaluated. The bonding characteristics of bispherical clusters are dominated by the bonding molecular orbitals of the inner polyhedron, but some additional skeletal bonding molecular orbitals may be generated from the L^x orbitals of the outer polyhedron. Spherical (or pseudo-spherical) clusters are created by distorting the bispherical clusters until all the atoms lie approximately on the surface of one sphere. These clusters are characterised by $(N + 1)$ skeletal electron pairs.

The Tensor Surface Harmonic Theory, developed by Stone,¹⁻⁴ constructs a set of approximate molecular orbitals from the solution of the Schrodinger equation for a particle on a sphere. The application of this methodology to deltahedral clusters has led to an elegant justification of the $(N + 1)$ skeletal electron-pair rule,² which is a central feature of the Polyhedral Skeletal Electron Pair Approach.⁵ Subsequently this methodology has been extended to three- and four-connected polyhedral molecules.^{6,7} The group theoretical aspects of these problems have been discussed by Ceulemans,⁸ Quinn and co-workers,⁹ Fowler,¹⁰ and ourselves.¹¹ As in other situations where the free-electron model works well, *e.g.* conjugated polyenes,¹² the ordering of energy levels is determined by the nodal characteristics of the orbitals rather than their detailed forms. Therefore, even within a semiempirical framework, such an approach predicts the correct ordering of molecular orbitals and, in particular, closed-shell requirements.¹³ Tensor surface harmonic theory is based on the assumption that all the cluster atoms lie on a single spherical surface and the ligands on a second concentric surface. In this paper the bonding in clusters which have metal atoms on several concentric spherical surfaces is discussed.

Results and Discussion

Bispherical Clusters.—Bispherical clusters are defined as those clusters having their two sets of symmetry-equivalent atoms lying on the surfaces of two concentric spheres of differing radii.¹⁴ The relationship between spherical (all atoms on the surface of the same sphere) and bispherical clusters is effectively demonstrated for a high-symmetry situation such as that shown in Figure 1. The rhombic dodecahedron has fourteen atoms effectively lying on a single sphere (actually the polyhedron is not quite spherical but there is an interior sphere which cuts all of its edges) and, therefore, its bonding can be analysed in terms of the (single-sphere) tensor surface harmonic theory. The analysis is also simplified by the octahedral symmetry of the polyhedron. Figure 1 also illustrates how two bispherical clusters of O_h symmetry can be generated from the rhombic dodecahedron, an octacapped octahedron and a hexacapped cube. Both of these bispherical clusters are examples of omnicauded polyhedra and are topologically related by the dual nature of the cube and the octahedron.

Topological Features of Bispherical Clusters.—Two polyhedra

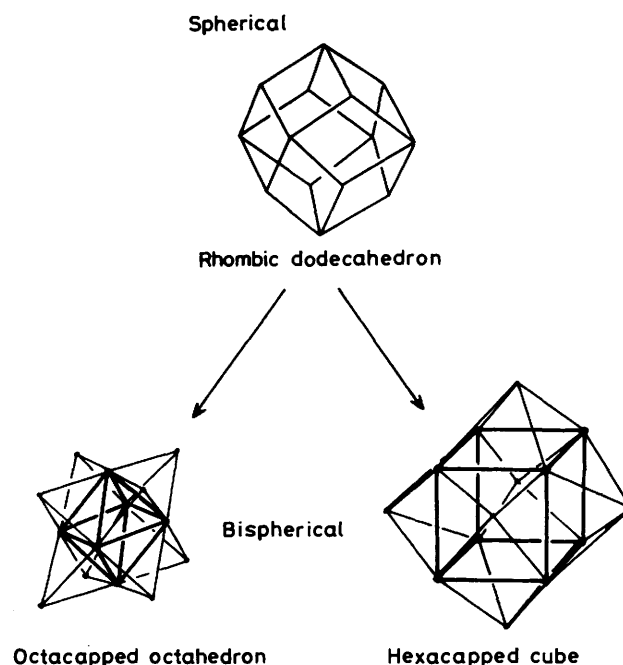


Figure 1. 14-Vertex spherical and bispherical polyhedra with octahedral symmetry

A and B are described as face-duals¹⁵ if the faces of A are replaced by vertices in B and *vice versa*. The polyhedra A and B belong to the same symmetry point group and the relationships between the number of vertices (V), faces (F), and edges (E) of the two dual polyhedra are $V_B = F_A$, $F_B = V_A$, and $E_B = E_A$, and the Euler relationship¹⁵ ($V + F = E + 2$) applies to both polyhedra.

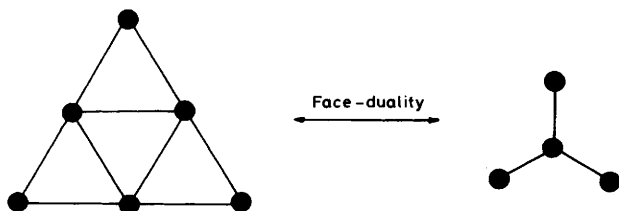
In the case under consideration polyhedron A is an octahedron, which is an example of a deltahedron as all of its faces are triangular. Its (face) dual B is a cube, which is a three-connected polyhedron as all of its vertices are connected to three others. In general the dual of a deltahedron, where each of the triangular faces has three neighbouring faces, is always a three-connected polyhedron, as illustrated in Figure 2. Since the dual relationship is reciprocal, the dual of a three-connected polyhedron must be a deltahedron. Figure 3 illustrates further examples of dual-related deltahedra and three-connected polyhedra.

† Part 1 is ref. 14.

The following relationships apply to deltahedra (subscript Δ) and three-connected polyhedra (subscript 3):

Deltahedra	Three-connected polyhedra
$F_{\Delta} = 2(V_{\Delta} - 2)$	$F_3 = (V_3/2) + 2$
$E_{\Delta} = 3(V_{\Delta} - 2)$	$E_3 = (3V_3/2)$
$E_{\Delta} = (3F_{\Delta}/2)$	$E_3 = 3(F_3 - 2)$

The number of vertices in an omnicailed deltahedron (V_{omni}) or omnicailed three-connected polyhedron is obviously the same when the deltahedron and three-connected polyhedron are duals: $V_{\text{omni}} = V_{\Delta} + V_3 = V_{\Delta} + F_{\Delta} = F_3 + V_3$, thus $V_{\text{omni}} = 3V_{\Delta} - 4 = (3V_3/2) + 2$.



Deltahedron (triangular faces) Three-connected polyhedron (trivalent vertices)

Figure 2. The face-duality relationship between deltahedra and three-connected polyhedra

The bispherical omnicailed polyhedra may be converted into spherical polyhedra by simultaneously expanding the inner sphere and contracting the outer sphere until all of the atoms lie on the same sphere. This does not change the point-group symmetry of the polyhedron since it is the radial and not the angular disposition of the cluster vertices which is changed by this process. In the spherical limit, $V_{\text{omni}} = V_{\text{sph}}$ and the above relationships apply, with V_{omni} replaced by V_{sph} . Since three-connected polyhedra must possess an even number of vertices, V_3 takes the values 4, 6, 8, 10, etc. which, from the equations above, results in V_{omni} (or V_{sph}) values of 8, 11, 14, 17, etc. Thus bispherical or spherical clusters, which are composites of a deltahedron and its three-connected dual, are characterised by $(3x + 5)$ atoms ($x = 1, 2, 3, \text{etc.}$). Examples of spherical clusters of this type are illustrated in Figure 4. It should be noted that these spherical polyhedra are all rhombohedra (possessing square or rhombic faces, $V_{\text{sph}} = V_{\diamond}$) and as such are the duals of four-connected polyhedra. The spherical clusters can be distorted in two distinct ways to generate bispherical clusters with either the deltahedron or its three-connected dual lying on the inner sphere.

Group Theoretical Analysis.—The molecular orbitals of the individual polyhedra in a bispherical cluster (inner and outer spheres) can, by employing the tensor surface harmonic methodology, be expressed as spherical harmonic expansions and assigned L^{σ} , L^{π} , \bar{L}^{π} ... quantum numbers. Rules for

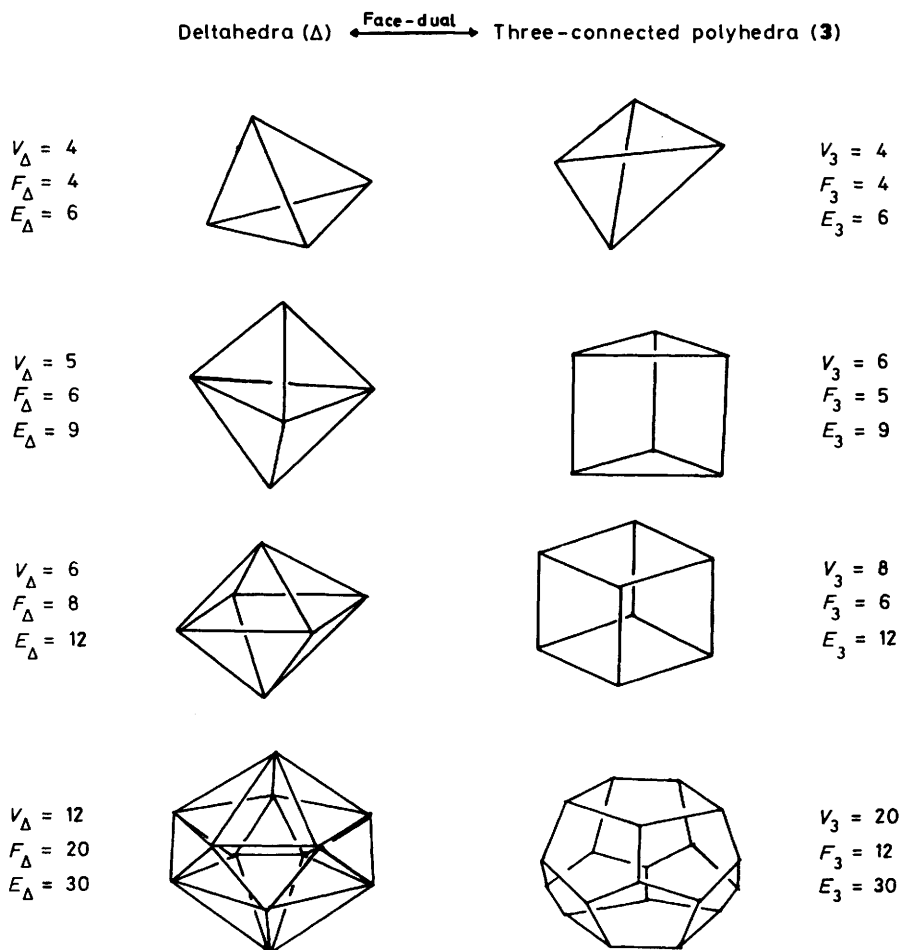
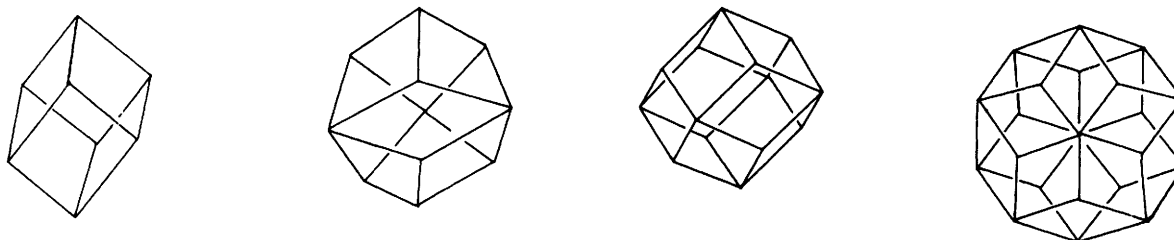


Figure 3. Some face-dual deltahedra and three-connected polyhedra



Cube (rhombic hexahedron)

$$V_{\diamond} = V_{\Delta}(4) + V_3(4) = 8$$

$$V_{\diamond} = 3X + 5 \quad (X = 1)$$

$$F_{\diamond} = V - 2 = E_{\Delta} = E_3 = 6$$

Rhombic enneaehedron

$$V_{\diamond} = V_{\Delta}(5) + V_3(6) = 11$$

$$X = 2$$

$$F_{\diamond} = 9$$

Rhombic dodecahedron

$$V_{\diamond} = V_{\Delta}(6) + V_3(8) = 14$$

$$X = 3$$

$$F_{\diamond} = 12$$

Rhombic triacontahedron

$$V_{\diamond} = V_{\Delta}(12) + V_3(20) = 32$$

$$X = 9$$

$$F_{\diamond} = 30$$

N.B. The number of faces (F_{\diamond}) of a rhombohedron is equal to the number of edges ($E_{\Delta} = E_3$) of its constituent (dual) polyhedra because the rhombohedra are the face-duals of the (four-connected) polyhedra derived by placing a vertex at the midpoint of each edge of the deltahedra or three-connected polyhedra (*i.e.* edge-duals).

$$E_{\diamond} = 2F_{\diamond} = E_{\Delta} + E_3 = 12$$

$$E_{\diamond} = 18$$

$$E_{\diamond} = 24$$

$$E_{\diamond} = 60$$

Figure 4. 'Spherical' rhombohedra as the composites of three-connected polyhedra and their dual deltahedra

Table 1. Symmetries of the spherical harmonics in some finite point groups

R_{3h}	I_h	O_h	T_d	D_3
$S_g^{\sigma}, (\Gamma_g^0)$	A_g	A_{1g}	A_1	A_1
P_u^{σ}, P_u^{π}	T_{1u}	T_{1u}	T_2	$A_2 + E$
D_g^{σ}, D_g^{π}	H_g	$E_g + T_{2g}$	$E + T_2$	$A_1 + 2E$
F_u^{σ}, F_u^{π}	$T_{2u} + G_u$	$A_{2u} + T_{1u} + T_{2u}$	$A_1 + T_1 + T_2$	$A_1 + 2A_2 + 2E$
G_g^{σ}, G_g^{π}	$G_g + H_g$	$A_{1g} + E_g + T_{1g} + T_{2g}$	$A_1 + E + T_1 + T_2$	$2A_1 + A_2 + 3E$
Γ_u^0	A_u	A_{1u}	A_2	A_1
\bar{P}_g^{π}	T_{1g}	T_{1g}	T_1	$A_2 + E$
\bar{D}_g^{π}	H_u	$E_u + T_{2u}$	$E + T_1$	$A_1 + 2E$
\bar{F}_g^{π}	$T_{2g} + G_g$	$A_{2g} + T_{1g} + T_{2g}$	$A_2 + T_1 + T_2$	$A_1 + 2A_2 + 2E$
\bar{G}_g^{π}	$G_u + H_u$	$A_{1u} + E_u + T_{1u} + T_{2u}$	$A_2 + E + T_1 + T_2$	$2A_1 + A_2 + 3E$

obtaining these orbitals, employing group theoretical techniques, are presented below.⁹⁻¹¹

(1) The reducible representation (Γ_{σ}) resulting from the permutation of radial (σ) orbitals, under the operations of the cluster point group, is decomposed into its constituent irreducible representations: $\Gamma_{\sigma} = a\Gamma_1 + b\Gamma_2 + c\Gamma_3$, *etc.*

(2) The L^{σ} labels are obtained by consulting a correlation table (see Table 1 for example) for the descent in symmetry from spherical (R_{3h}) to the appropriate cluster point-group symmetry. The lowest L values are chosen which generate all the constituent irreducible representations of Γ_{σ} .

(3) The irreducible representations spanned by the L^{π} and \bar{L}^{π} orbitals are obtained from those of the L^{σ} orbitals⁹ by the relationship (1) where \otimes indicates tensor multiplication.

$$\Gamma_{\pi+\bar{\pi}} = \{\Gamma_{\sigma} \otimes \Gamma_{x,y,z}\} - \Gamma_{\sigma} \quad (1)$$

This equation derives from the fact that at any atom position linear combinations of p_x , p_y , and p_z atomic orbitals may be taken so as to generate one radial (p^{σ}) and two tangential ($2p^{\pi} = p^{\theta} + p^{\phi}$) components. In axial point groups this equation may be simplified as in (2) and (3) (where R_z indicates

$$\Gamma_{\pi+\bar{\pi}}^0 = \Gamma_{\sigma} \otimes \Gamma_z \quad (2)$$

$$\Gamma_{\pi+\bar{\pi}}^{\sigma} = \{\Gamma_{\sigma} \otimes \Gamma_z\} \otimes \Gamma_u^0 = \Gamma_{\sigma} \otimes \Gamma_{R_z} \quad (3)$$

rotation about the z axis),¹¹ provided that there are no axial atoms (as p_z becomes purely radial in character on the principal rotation axis); Γ_u^0 is the irreducible representation (which is

symmetric with respect to all proper rotations of the point group but antisymmetric with respect to all improper rotations) corresponding to the parity-inversion operation ($\hat{\epsilon}$)¹ which interconverts L^{π} and \bar{L}^{π} : $L^{\pi} \xleftrightarrow{\hat{\epsilon}} \bar{L}^{\pi}$. For clusters, belonging to axial point groups, possessing no atoms in the equatorial plane (with or without axial atoms) the relevant equation is (4).

$$\Gamma_{\pi+\bar{\pi}} = \Gamma_{\sigma} \otimes \Gamma_{x,y} \quad (4)$$

Once the irreducible representations spanned by the tangential orbitals ($\Gamma_{\pi+\bar{\pi}}$) are known then the L^{π} and \bar{L}^{π} orbitals are obtained by consulting a correlation table (Table 1) which includes \bar{L}^{π} as well as L^{π} ($\Gamma_{\bar{\pi}} = \Gamma_{\pi} \otimes \Gamma_u^0$). The L^{π} and \bar{L}^{π} functions must be equal in number and parity related.

(4) Finally for bi- or multi-spherical clusters (Z), or spherical clusters consisting of two or more distinct sets of symmetry-equivalent atoms (A, B, C , *etc.*), the irreducible representations spanned by L^{σ} and L^{π}/\bar{L}^{π} are obtained by summing those of the constituent polyhedra. For example, $\Gamma_{\sigma}(Z) = \Gamma_{\sigma}(A) + \Gamma_{\sigma}(B) + \Gamma_{\sigma}(C) + \text{etc.}$ Again a correlation table, such as Table 1, is used to evaluate the L values for the L^{σ} , L^{π} , and \bar{L}^{π} orbitals of the multispherical cluster. The principle of always taking the lowest possible L values may lead to L^{π} orbitals of the multispherical cluster which are not symmetry matched by the L^{σ} orbitals of its constituent polyhedra. Instead these orbitals correspond to combinations of \bar{L}^{π} orbitals of the constituent polyhedra. The parity-inversion operation ensures that there will be a parity-related combination of L^{π} orbitals which end up as \bar{L}^{π} for the multispherical cluster.

Taking the rhombic dodecahedron as an example (the

symmetries of the orbitals of the hexacapped cube and the octacapped octahedron will be identical), the L^σ , L^π , and \bar{L}^π orbitals of its constituent polyhedra (cube and octahedron) may be evaluated. For the cube, $\Gamma_\sigma(\text{cube}) = a_{1g} + t_{1u} + t_{2g} + a_{2u}$ and $\Gamma_{\pi+\bar{\pi}}(\text{cube}) = t_{1u} + t_{2g} + e_g + t_{1g} + t_{2u} + e_u$. The cube possesses 12 skeletal electron pairs,⁶ $S^\sigma(a_{1g}) + P^{\sigma+\pi}(t_{1u}) + D^\pi(e_g + t_{2g}) + \bar{D}^\pi(t_{2u})$ (see Table 2), six of which are in roughly non-bonding orbitals, $D^\pi(t_{2g}) + \bar{D}^\pi(t_{2u})$. The occupied skeletal molecular orbitals are topologically equivalent to the 12 edges of the cluster and can be alternatively generated as linear combinations of edge-bonding (nodeless) localised orbitals. The unoccupied orbitals, on the other hand, may be expressed as linear combinations of edge-antibonding (singly noded) localised orbitals. In general a three-connected poly-

hedron has $3V_3/2 (= E_3)$ skeletal electron pairs, $(V_3 - 2)$ of which are non-bonding [made up of $(V_3/2) - 1$ L^π orbitals and their $(V_3/2) - 1$ \bar{L}^π parity-inverted counterparts].⁶ For the octahedron, $\Gamma_\sigma(\text{octahedron}) = a_{1g} + t_{1u} + e_g$ and $\Gamma_{\pi+\bar{\pi}}(\text{octahedron}) = t_{1u} + t_{2g} + t_{1g} + t_{2u}$. The octahedron, as a deltahedron, possesses seven $(= V_\Delta + 1)$ skeletal bonding molecular orbitals, $S^\sigma(a_{1g}) + P^{\sigma+\pi}(t_{1u}) + D^\pi(t_{2g})$ (see Table 2), and no non-bonding orbitals. Finally, for the rhombic dodecahedron, $\Gamma_\sigma(\text{rhombic dodec.}) = 2a_{1g} + 2t_{1u} + t_{2g} + e_g + a_{2u}$ and $\Gamma_{\pi+\bar{\pi}}(\text{rhombic dodec.}) = 2t_{1u} + 2t_{2g} + 2t_{1g} + 2t_{2u} + e_g + e_u$. Employing Table 1, L values may be assigned to the above orbitals, yielding the results shown in Table 2. It should be noted that the two sets (one from the cube and one from the octahedron) of $\bar{D}^\pi(t_{2u})$ orbitals give rise, in the rhombic dodecahedron, to one set of odd parity (\bar{D}^π) and one set of even parity (F^π). Similarly the t_{2g} orbitals give rise to D^π and F^π combinations.

Table 2. The L^σ , L^π , and \bar{L}^π orbitals (and their symmetries) of the cube, octahedron, and rhombic dodecahedron (O_h symmetry)

L^σ	Cube	Octahedron	Rhombic dodecahedron
S^σ	A_{1g}	A_{1g}	A_{1g}
P^σ	T_{1u}	T_{1u}	T_{1u}
D^σ	T_{2g}	E_g	$E_g + T_{2g}$
F^σ	A_{2u}		$A_{2u} + T_{1u}$
G^σ			A_{1g}
L^π			
P^π	T_{1u}	T_{1u}	T_{1u}
D^π	$E_g + T_{2g}$	T_{2g}	$E_g + T_{2g}$
F^π			$T_{1u} + T_{2u}$
\bar{L}^π			
\bar{P}^π	T_{1g}	T_{1g}	T_{1g}
\bar{D}^π	$E_u + T_{2u}$	T_{2u}	$E_u + T_{2u}$
F^π			$T_{1g} + T_{2g}$

Inner Sphere-Outer Sphere Interactions.—In the limit of no interaction between the orbitals of the outer and inner spheres (for instance when the outer-sphere radius tends to infinity) the spectrum of molecular orbitals of the bispherical cluster is identical to that of the isolated inner-sphere polyhedron plus additional degenerate non-bonding orbitals belonging to the outer-sphere polyhedron. Figure 5 illustrates these non-interacting bispherical extremes for the octacapped octahedron and the hexacapped cube. The cluster atoms possess three valence orbitals (1 σ -type and 2 π -type) which give rise to cluster molecular orbitals of the type L^σ , L^π , and \bar{L}^π . In this limit the omnicailed deltahedron is characterised by $(V_\Delta + 1)$ skeletal bonding molecular orbitals and the omnicailed three-connected polyhedron by $(3V_3/2)$ skeletal bonding molecular orbitals.^{2,6}

As the outer-sphere radius is reduced the molecular orbitals of the inner- and outer-sphere polyhedra (with matching

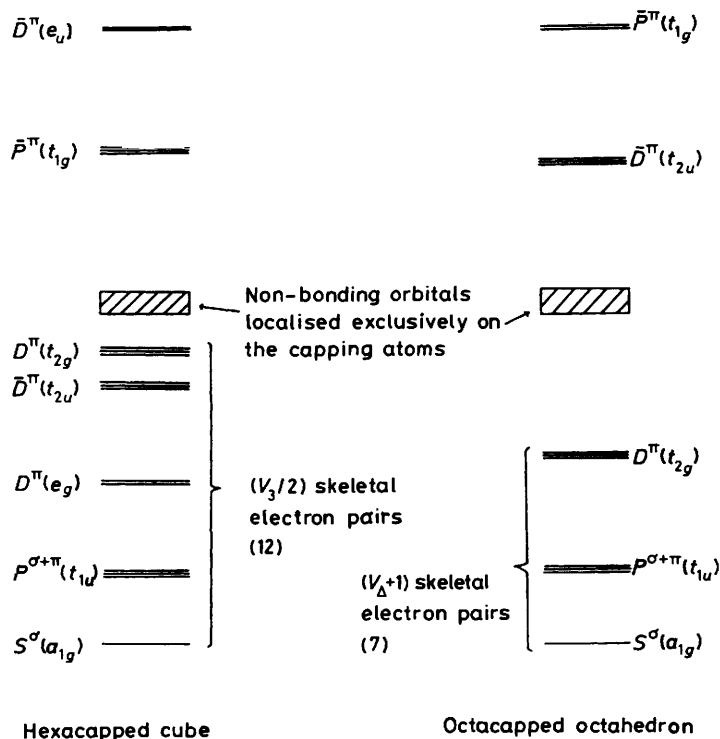


Figure 5. Molecular orbital schemes for the bispherical extremes of the hexacapped cube and the octacapped octahedron, with no interaction between the orbitals of the inner- and outer-sphere polyhedra

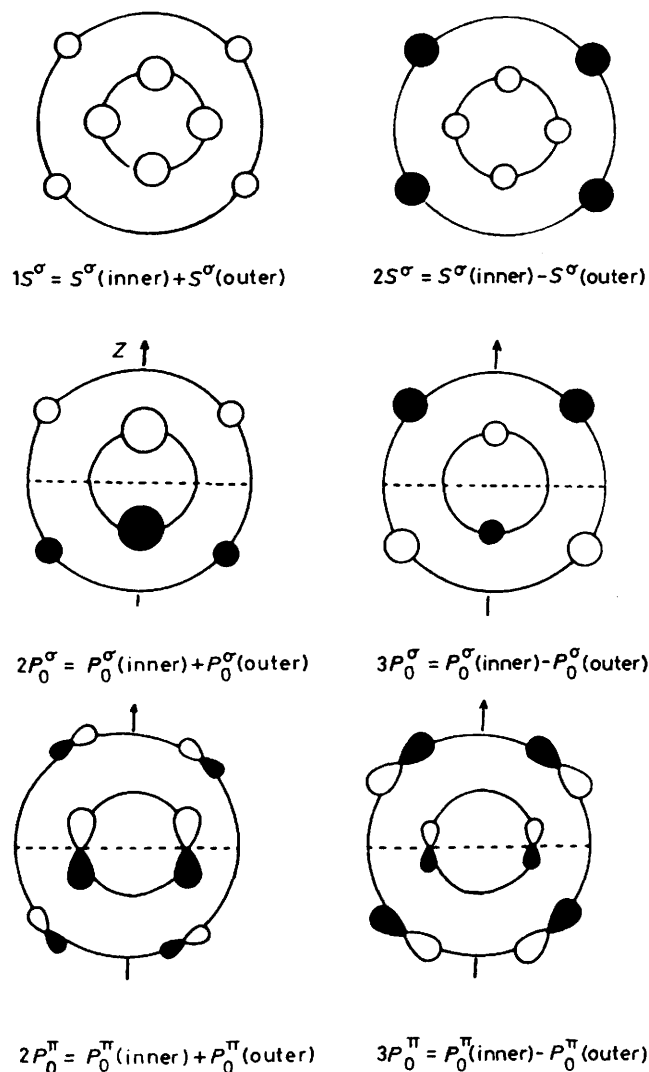


Figure 6. Bispherical tensor surface harmonic wavefunctions (L^σ and L^π) possessing radial as well as angular nodes

symmetry characteristics) begin to interact. The effect of this interaction is to introduce radial as well as tangential nodes into the cluster wavefunctions. The primary interactions correspond to the overlap of inner- and outer-sphere molecular orbitals having matching L quantum numbers. Figure 6 illustrates these interactions for L^σ and L^π orbitals of a generalised bispherical cluster and emphasises how additional radial nodes are introduced. Generalised molecular-orbital interaction diagrams, for L^σ , L^π (and \bar{L}^π) orbitals, are presented in Figure 7. Since the atoms of the outer-sphere polyhedron are further apart than those of the inner sphere, the spread of molecular orbitals is narrower for the outer sphere. For L^σ and L^π this generally results in the in-phase combinations being predominantly localised on the inner sphere while the radially noded antibonding combinations are predominantly localised on the outer sphere (see Figure 6 for example). For L^σ orbitals with high L values, however, the orbitals of the inner sphere are high in energy due to the large number of angular nodes in the wavefunction, thus the in-phase inner sphere-outer sphere combination is predominantly localised on the outer-sphere atoms. The \bar{L}^π orbitals are generally more antibonding for the inner than the outer sphere so their bonding combination (see Figure 7) is mainly localised on the outer sphere.

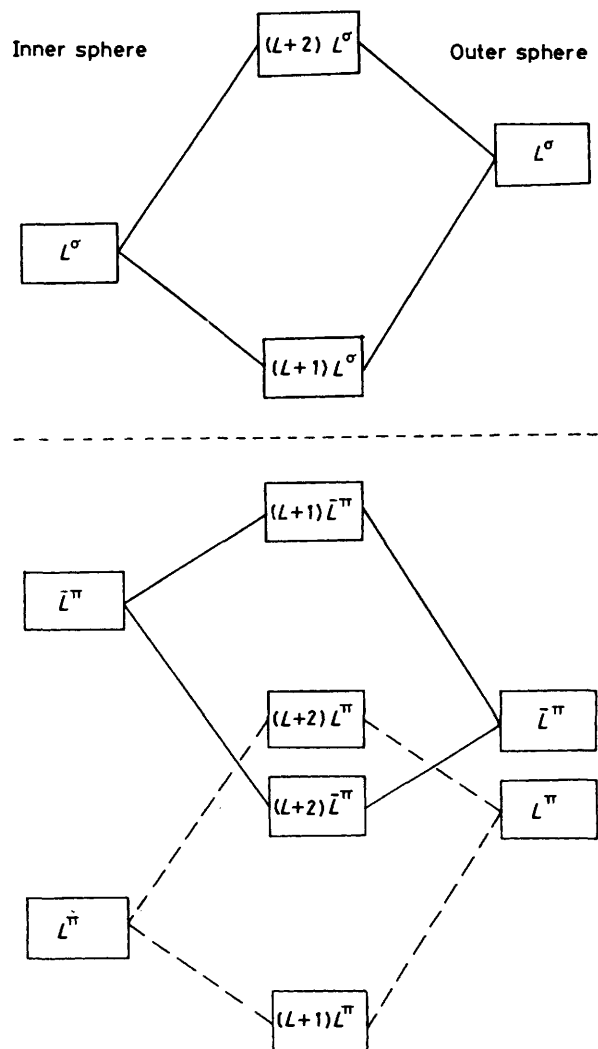


Figure 7. Interaction between orbitals of the inner- and outer-sphere polyhedra in bispherical clusters. The 'cluster orbital principal quantum number' is given in parentheses; thus the interaction of $S^\sigma(\text{inner})$ and $S^\sigma(\text{outer})$ ($L = 0$) yields the bonding orbital $1S^\sigma$ and the antibonding orbital $2S^\sigma$

The nomenclature employed follows that for atomic orbitals, thus the $1S^\sigma$ cluster orbital possesses no radial nodes while $2S^\sigma$ and $3S^\sigma$ (needed in a trispherical cluster) possess one and two radial nodes respectively. Similarly, $2P^\sigma$ and $2P^\pi$ possess no radial nodes and $3P^\sigma$ and $3P^\pi$ have one radial node. In general $nL^{\sigma,\pi}$ has $(n - L - 1)$ radial nodes, as for atomic orbitals. In this context it is interesting that the atomic orbital property that the maximum in the radial part of the wavefunction moves to greater radius as n increases is neatly mimicked in our model (at least for L^σ orbitals with low L values) by the localisation of the maximum of electron density on successively larger spheres as the n quantum number increases (see Figure 6 for example).

Upon interaction of the L^σ and L^π orbitals of the inner and outer spheres, the resulting orbital with the fewer radial nodes (lowest n) is more strongly bonding. As a result of the parity-inversion operation ($\hat{\epsilon}$) which relates L^π and $L^{\pi 1}$ and interconverts their bonding characteristics,³ the opposite situation applies for the L^π orbitals of a bispherical cluster, *i.e.* the greater the number of radial nodes (higher n) the lower is the energy of nL^π . These conclusions are summarised in Figure 7.

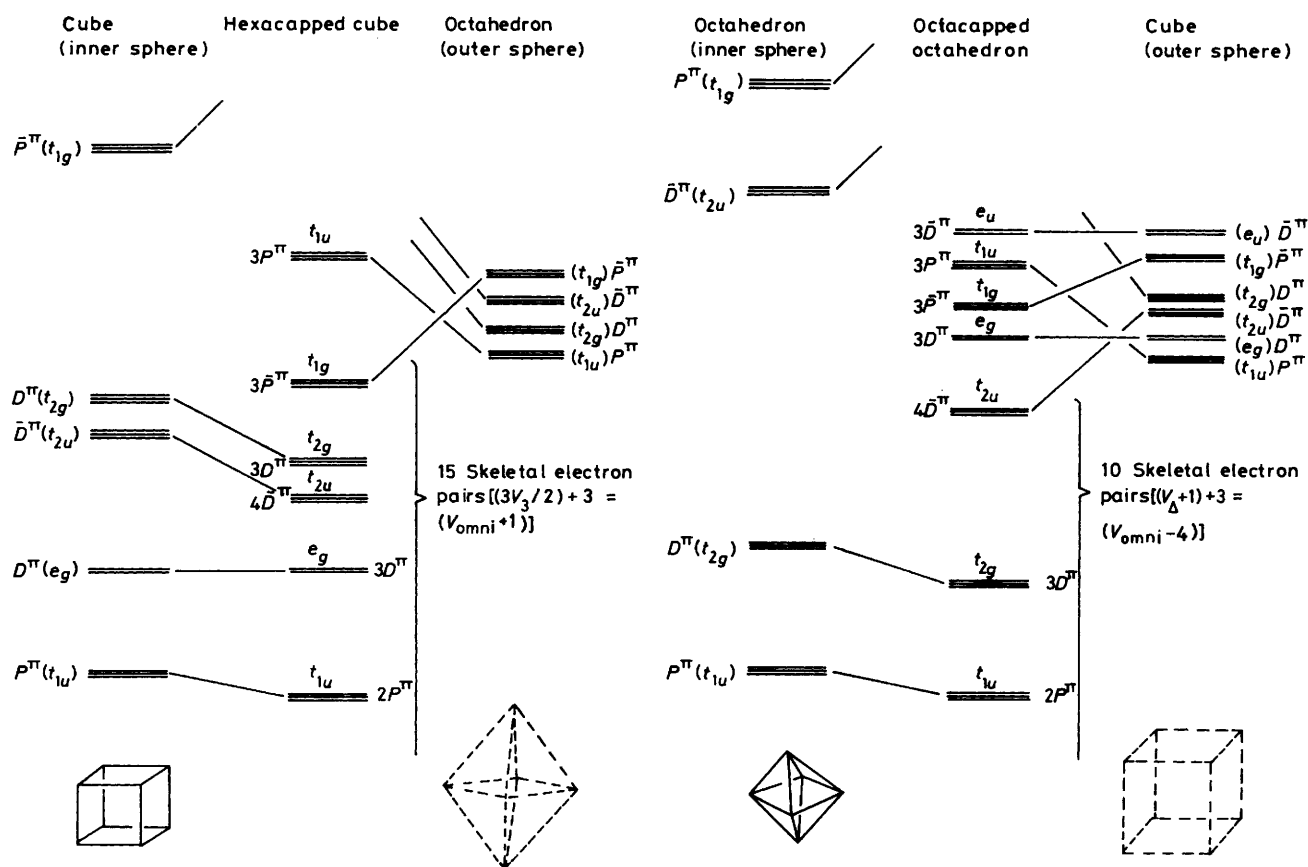


Figure 8. Molecular orbital (inner sphere-outer sphere) interaction diagrams for the hexacapped cube and the octacapped octahedron

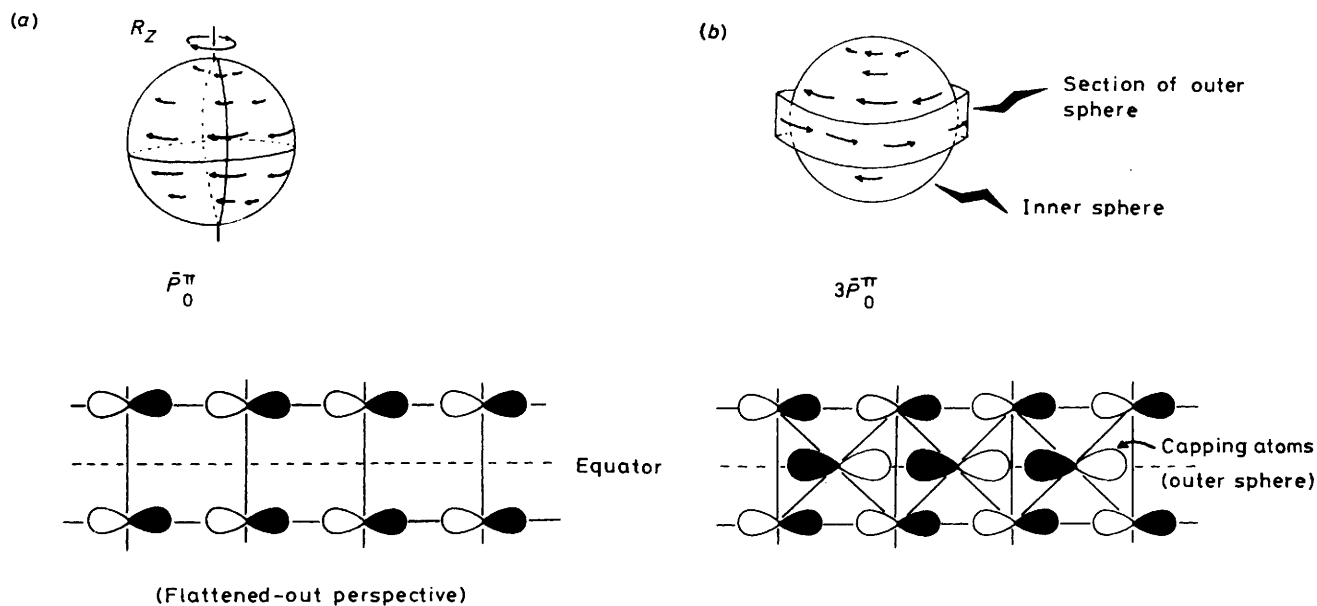


Figure 9. The \bar{P}_0^π orbitals for spherical and bispherical clusters based on a prismatic (three-connected) inner-sphere polyhedron

The consequences of these inner sphere-outer sphere interactions are shown in Figure 8 for the omnicailed octahedron and cube. An important feature to note is that in both cases the interaction leads effectively to stabilisation of the bonding orbitals of the inner-sphere polyhedron and corre-

sponding destabilisation of those of the outer sphere. In itself this would lead to no change in the number of skeletal electron pairs, which is indeed observed when polyhedra are capped on only a few of their faces (*i.e.* when there are not many atoms on the outer sphere) and forms the basis of the capping principle.¹⁶

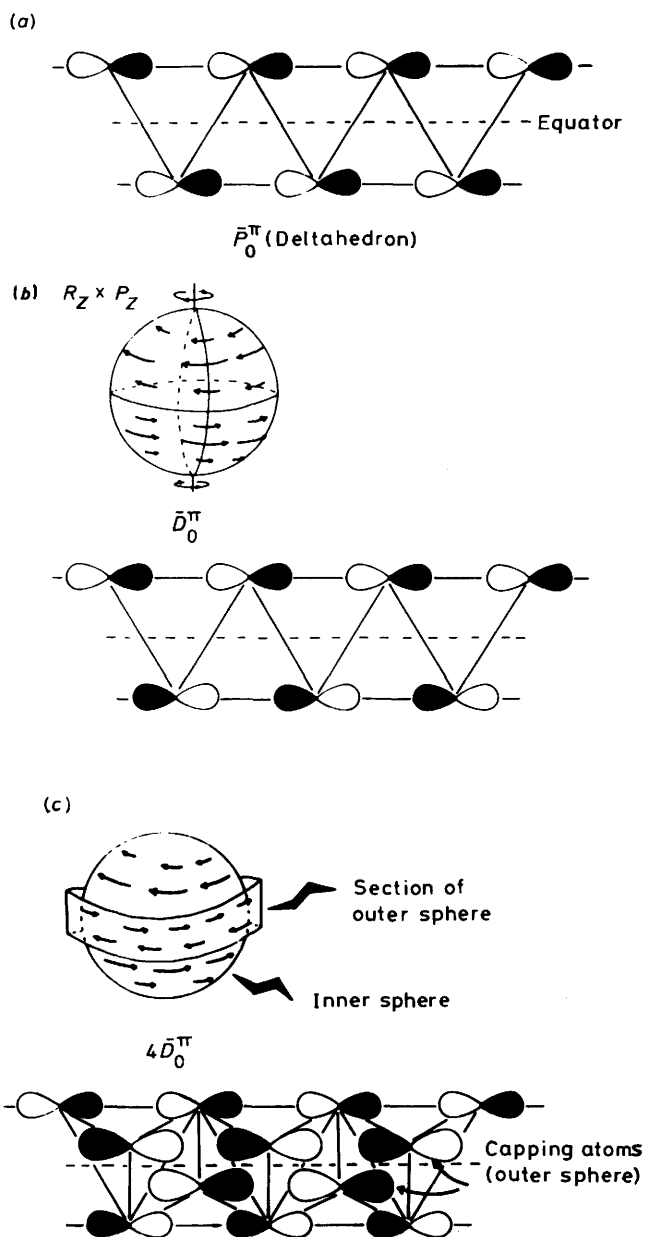


Figure 10. The \bar{P}_0^π and \bar{D}_0^π orbitals for spherical and bispherical clusters based on an antiprismatic (deltahedral with respect to the equator) inner-sphere polyhedron

When the capping atoms form a complete polyhedron, however, the bonding combination of certain of the \bar{L}^π orbitals may be sufficiently low in energy to be occupied. For three-connected polyhedra the \bar{L}^π orbitals of interest are \bar{P}^π . As shown in Figure 8 the three $3\bar{P}^\pi(t_{1g})$ orbitals of the hexacapped cube possess overall bonding character. Three-connected polyhedra, in general, have the \bar{P}^π orbitals as the lowest unoccupied molecular orbitals (l.u.m.o.s) because of the π -bonding interaction they exhibit across the equatorial plane. Figure 9(a) illustrates this bonding interaction for one component of the \bar{P}^π orbitals (\bar{P}_0^π). When a ring of capping atoms (outer sphere) is introduced (creating a toroidal topology for the bispherical cluster) their \bar{P}_0^π orbital interacts strongly with that of the three-connected polyhedron to create a slightly bonding $3\bar{P}_0^\pi$ orbital [Figure 9(b)]. In the case of an omnicauded three-connected

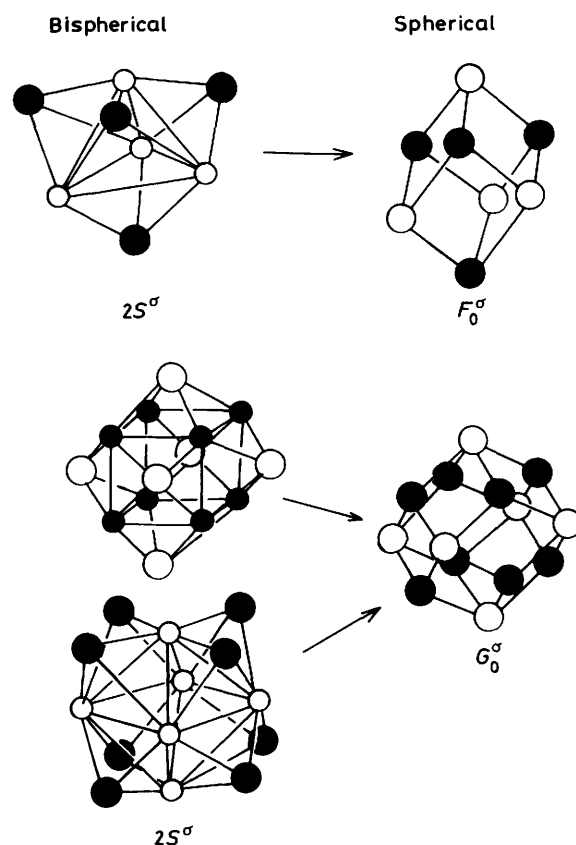


Figure 11. The conversion of radial nodes (in cluster molecular orbitals) into additional angular nodes on going from bispherical to spherical topology

polyhedron this process is repeated (in three perpendicular planes) for all three \bar{P}^π orbitals and three extra skeletal bonding molecular orbitals result which become the highest occupied molecular orbitals (h.o.m.o.s). This leads to a skeletal electron-pair count of $(3V_3/2) + 3$ for omnicauded three-connected polyhedra (15 for the hexacapped cube). The parity-related $3\bar{P}^\pi$ orbitals (antibonding combination of P^π on the two spheres) are the l.u.m.o.s. Generally these orbitals are fairly low lying and, therefore, potentially accessible.

The \bar{P}^π orbitals are more strongly antibonding for deltahedra than for three-connected polyhedra because, as shown in Figure 10(a), the interaction across the equator is antibonding rather than bonding. The l.u.m.o.s of the octahedron are $\bar{D}_{0,\pm 1}^\pi$ (with the octahedron viewed down the three-fold axis). Figure 10(b) illustrates the \bar{D}_0^π orbital of a deltahedron which is now bonding across the equator (it is strongly antibonding for a three-connected prism). As Figure 10(c) shows, overlap of this orbital with the \bar{D}_0^π orbital of the outer sphere will lead to a significant bonding interaction. When this interaction is repeated in three dimensions all three $\bar{D}_{0,\pm 1}^\pi$ orbitals interact strongly to yield three additional bonding orbitals ($4\bar{D}_{0,\pm 1}^\pi - t_{2u}$) and a total of $(V_\Delta + 4 = 10)$ skeletal electron pairs for the octacapped octahedron (see Figure 8).

Intermediate between these two extremes of bispherical clusters lies the spherical cluster, where all of the cluster atoms lie on the surface of the same sphere. Because the cluster is spherical its molecular orbitals may be adequately described in terms of spherical harmonic functions (L^σ , L^π , \bar{L}^π , etc.) with no radial nodes. Figure 11 shows that, on merging the inner and outer spheres to create a spherical cluster, radial nodes are

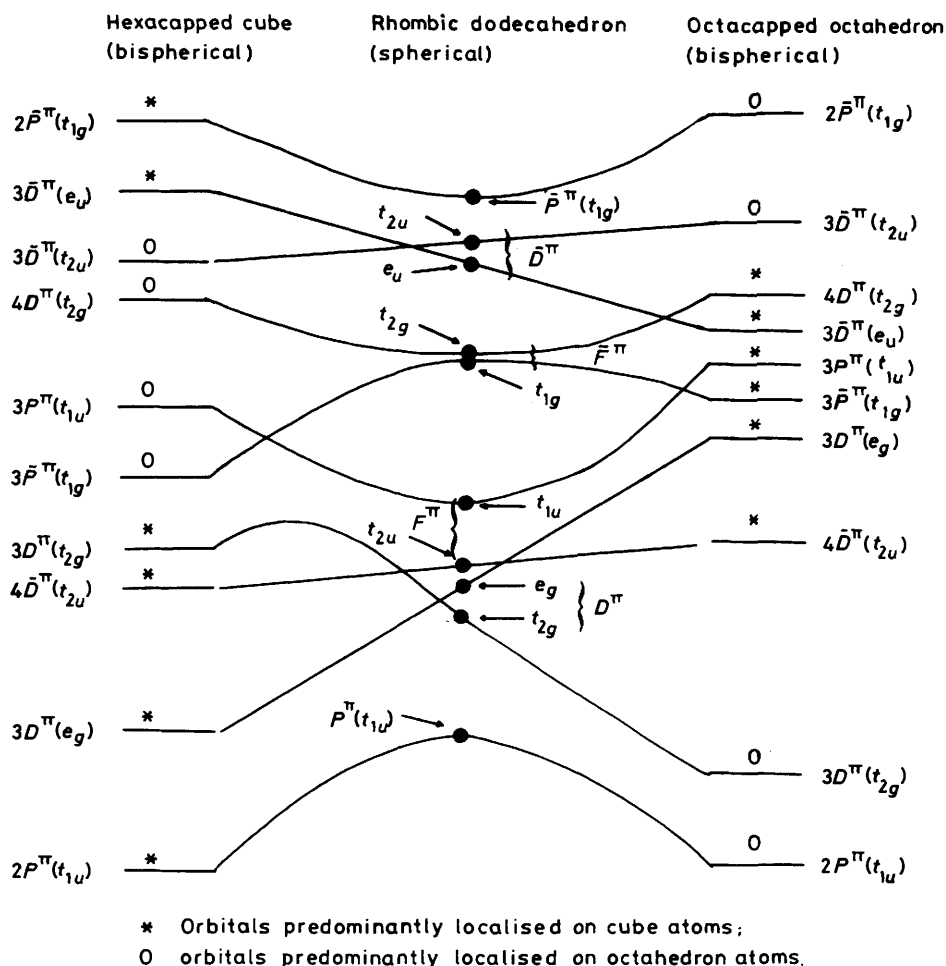


Figure 12. Correlation of the (L^* and \bar{L}^*) skeletal molecular orbitals of the (spherical) rhombic dodecahedron with those of the two bispherical extremes (hexacapped cube and octacapped octahedron)

Table 3. Rhombohedral clusters as the topological composites of three-connected polyhedra and their deltahedral duals (s.e.p. = skeletal electron pair)

Three-connected polyhedron (3)	Deltahedron (Δ)	Rhombohedral (\diamond) (Figure 4)
Tetrahedron ($V_3 = 4$) 6 ($3V_3/2$) s.e.p. e.g. $[\text{Ir}_4(\text{CO})_{12}]^a$	Tetrahedron ($V_\Delta = 4$) 6 s.e.p. e.g. $[\text{Os}_4(\text{CO})_{12}]^d$	Cube ($V_\diamond = 8$) 12 [$(3V_3/2) + 6$] s.e.p. $[\text{Ni}_8(\text{PPh})_6(\text{CO})_8]^b$
Trigonal prism ($V_3 = 6$) 9 ($3V_3/2$) s.e.p. e.g. $[\text{Rh}_6\text{C}(\text{CO})_{15}]^{2-c}$	Trigonal bipyramid ($V_\Delta = 5$) 6 s.e.p. ($V_\Delta + 1$) $[\text{Os}_5(\text{CO})_{15}]^d$	Rhombic enneahedron ($V_\diamond = 11$) 12 [$(3V_3/2) + 3$] s.e.p.
Cube ($V_3 = 8$) 12 ($3V_3/2$) s.e.p. e.g. $[\text{Ni}_8(\text{PPh})_6(\text{CO})_8]^b$	Octahedron ($V_\Delta = 6$) 7 s.e.p. ($V_\Delta + 1$) $[\text{Os}_6(\text{CO})_{18}]^{2-e}$	Rhombic dodecahedron ($V_\diamond = 14$) 15 [$(3V_3/2) + 3$] s.e.p. $[\text{Rh}_{15}(\text{CO})_{30}]^{3-f}$

^a M. R. Churchill and J. P. Hutchinson, *Inorg. Chem.*, 1978, 17, 3528. ^b L. D. Lower and L. F. Dahl, *J. Am. Chem. Soc.*, 1976, 98, 5046. ^c V. G. Albano, D. Braga, and S. Martinengo, *J. Chem. Soc., Dalton Trans.*, 1981, 717. ^d C. R. Eady, B. F. G. Johnson, J. Lewis, B. E. Reichert, and G. M. Sheldrick, *J. Chem. Soc., Chem. Commun.*, 1976, 271. ^e M. McPartlin, C. R. Eady, B. F. G. Johnson, and J. Lewis, *J. Chem. Soc., Chem. Commun.*, 1976, 883. ^f Ref. 17.

converted into extra angular nodes. The L values of the resulting orbitals depend critically on the disposition of the atoms and, in particular, the number of layers of atoms in the structure.

A diagram correlating the molecular orbitals of the octacapped octahedron (bispherical), rhombic dodecahedron (spherical), and hexacapped cube (bispherical) is presented in

Figure 12. A notable feature is the transformation (in both cases) of the bonding character of $3P^*$ and $3\bar{P}^*$ on going from the bispherical to the spherical topology. In the spherical cluster the $3P^*$ orbitals become bonding (F^*) while the $3\bar{P}^*$ orbitals become antibonding (\bar{F}^*). Going from the hexacapped cube to the rhombic dodecahedron there is, therefore, no change in the number of skeletal electron pairs, $(3V_3/2) + 3 = V_{\text{sp}} + 1$ [since

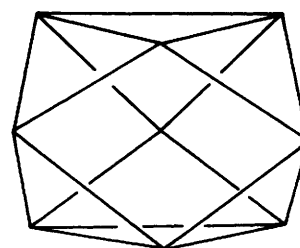
$V_{\text{sph}} = (3V_3/2) + 2$] and the spherical polyhedron has the expected $(N + 1)$ skeletal electron-pair count.⁷ On going from the octacapped octahedron to the rhombic dodecahedron five extra orbitals become bonding: $D^*(e_g)$, localised exclusively on the cube atoms) and $3P^*$ [becoming $F^*(t_{1u})$]. The cluster $[\text{Rh}_{15}(\text{CO})_{30}]^{3-}$ has a rhombic dodecahedral structure, with an additional metal atom at the centre of the cluster.¹⁷ It possesses 198 cluster valence electrons, corresponding to the occupation of 15 $(N + 1)$, where N is the number of surface atoms) skeletal bonding molecular orbitals and $(14N + 2)$ electrons. The $(14N + 2)$ count comes from $(2N + 2)$ skeletal bonding electrons and 12 electrons per (outer) metal which are either non-bonding (localised on the metals) or involved in metal-ligand bonding.⁵ The presence of an interstitial metal atom effectively leads to another type of bispherical cluster with atoms or cluster units completely enclosed by an outer sphere of metal atoms. Such encapsulated clusters have been discussed by Mingos¹⁸ and will be the subject of a subsequent publication.¹⁹ The orbitals of the interstitial atom interact with those of the cluster in such a way that its electrons are donated to the cluster. The presence of interstitial atoms will, of course, stabilise more spherical structures by way of strong radial bonds to the outer atoms.

As mentioned above, omnicaapping a three-connected polyhedron leads to a bispherical cluster with $3P^*$ and $3\bar{P}^*$ in the frontier-orbital region. On omnicaapping a tetrahedral cluster (six skeletal electron pairs) and then distorting the bispherical cluster, so that all the atoms lie on the surface of the same sphere, a cube (rhombic hexahedron) is formed. Cubic clusters (O_h symmetry) are characterised by 12 skeletal electron pairs and the six 'additional' electron pairs occupy orbitals [$D^*(t_{2g})$ and $\bar{D}^*(t_{2u})$] which are roughly non-bonding⁶ and which correspond to the $3P^*(t_2)$ and $3\bar{P}^*(t_1)$ orbitals of the (bispherical) tetracapped tetrahedron (T_d). This should be contrasted with the rhombic dodecahedron which only possesses three skeletal electron pairs in excess of the 12 possessed by the cube, from which it is derived. Table 3 gives examples of three-connected clusters and their (spherical) rhombohedral derivatives, which may be regarded as distorted omnicaapping (bispherical) three-connected polyhedra.

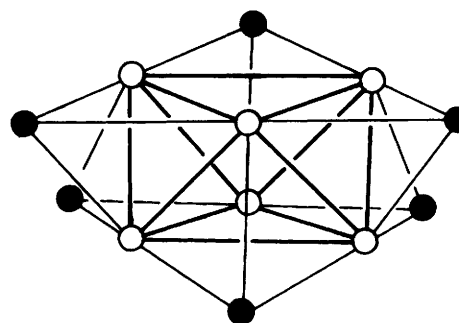
Bispherical Clusters with Toroidal Topologies.—So far the discussion has concerned omnicaapping polyhedral structures. Other types of bispherical polyhedra are possible, however, where the outer sphere may consist of a number of atoms which is less than the number of faces of the inner polyhedron. Such examples include edge-bridged polyhedra and capped (but not omnicaapping) polyhedra.

The tricapped trigonal prism is the simplest example of a three-connected cluster which has a planar ring of capping atoms around the equator (*i.e.* only one plane of the outer sphere is utilised) thereby possessing a toroidal rather than spherical topology. As mentioned in the previous discussion and elsewhere,¹⁴ the interaction between the \bar{P}^* orbitals of the two spheres leads to one component of $3\bar{P}^*(3\bar{P}_0^*)$ becoming weakly bonding while $3P_0^*$ is weakly antibonding. On forming the spherical (four-connected) polyhedron (1), by stretching the trigonal prism and pushing in the capping atoms, these two orbitals cross over to make F_0^* (bonding) and \bar{F}_0^* (antibonding),⁶ so that both the bispherical cluster and the spherical cluster possess the same number of skeletal electron pairs: $(3V_3/2) + 1 = V_3 + (V_3/2) + 1$ (*i.e.* $V_{\text{sph}} + 1$), where $(V_3/2)$ is the number of capping atoms around the equator. A similar situation pertains to the tetracapped cube (with D_{4h} symmetry) which can be distorted into the four-connected spherical cuboctahedron (note here the symmetry is actually increased to O_h) with 13 $(N + 1)$ skeletal electron pairs.⁷

Capping an octahedron around the equator yields a



(1)

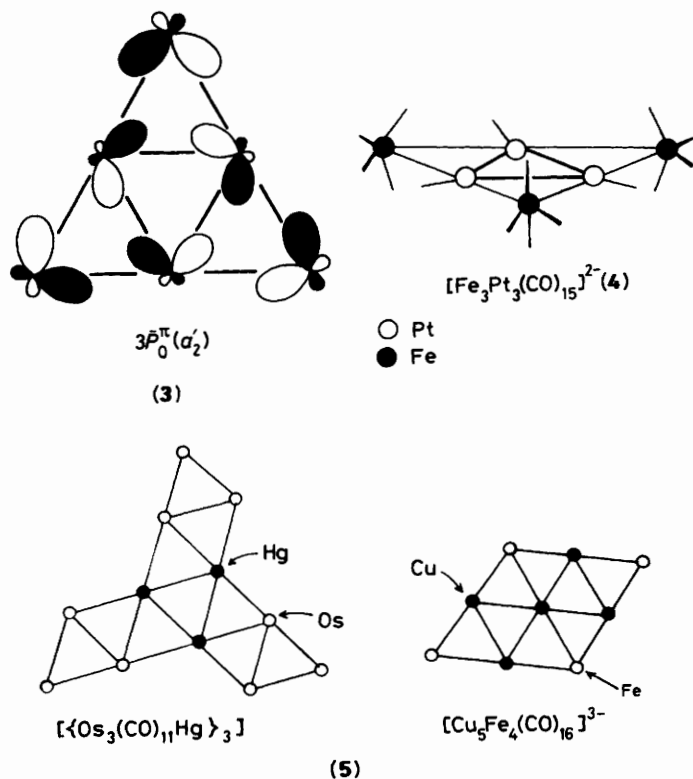
 $[\text{Fe}_6\text{Pd}_6(\text{CO})_{24}\text{H}]^{3-}$ (2)

bispherical cluster with an outer sphere of six atoms forming a puckered ring. By analogy with the omnicaapping octahedron, it is apparent that only one component ($4\bar{D}_0^*$) of the $4\bar{D}^*$ orbitals is sufficiently bonding to be occupied and a polyhedron with eight $(V_\Delta + 2)$ skeletal electron pairs results. An example of such a cluster is $[\text{Fe}_6\text{Pd}_6(\text{CO})_{24}\text{H}]^{3-}$ (2).²⁰ Examples of capped polyhedral clusters, where the capping atoms adopt polyhedral or polygonal (planar or puckered) arrangements and where certain \bar{L}^* orbitals may be sufficiently stabilised to be occupied, are given in Table 4. In agreement with the theoretical analysis, those clusters which have an incomplete set of capping atoms either possess the same number of skeletal bonding molecular orbitals as the parent polyhedra or have an additional electron pair occupying one component of \bar{L}^* . The only clusters which do not appear to conform to this analysis are $[\text{Ni}_{16}\text{C}_4(\text{CO})_{23}]^{4-}$ and $[\text{Pd}_{23}(\text{CO})_{22}(\text{PET}_3)_{10}]$ (see Table 4). The Ni_{16} cluster has a distorted tetracapped cuboctahedral structure and has four skeletal electron pairs in addition to the 13 characteristic of a cuboctahedral cluster. The distortion in this instance may be sufficient for this cluster to be classified as spherical with $(N + 1 = 17)$ skeletal electron pairs. The Pd_{23} cluster has a trispherical geometry based on a centred cuboctahedron which is capped on all its square faces, so that the capping atoms define an octahedron, and has a set of four edge-bridging PdL_2 groups. If these edge-bridging groups donate two electrons to the cluster (thereby forming localised two-centre two-electron bonds to the central cuboctahedral unit) the bispherical cluster which remains would be expected, from the analysis developed above, to have 16 skeletal electron pairs. This electron-pair count corresponds to the occupation of the 13 skeletal bonding orbitals of the cuboctahedron and three orbitals which are the bonding combinations of $\bar{D}_{\pm 1, -2}^*(t_{2u})$ (with the orbitals defined relative to a C_4 axis) on the cuboctahedron and the octahedron [$4\bar{D}^*(t_{2u})$]. The Pd_{23} cluster, however, actually possesses 15 skeletal electron pairs, which is attributable to the lowering of

symmetry (to D_{4h}), due to the presence of the four edge-bridging palladium atoms, and the consequent splitting of the $\bar{D}^n(t_{2u})$ orbitals into e_u and b_{2u} .

In those clusters where a ring of capping atoms exists but no 'new' skeletal bonding orbitals are introduced facile two-electron electrochemical reduction processes might reasonably be expected.

Raft Clusters.—Raft clusters²¹ may be described as a subclass of bi- (or multi-) spherical clusters with all of the atoms of the



inner and outer spheres lying on concentric rings in the same plane. Evans and Mingos²² identified the l.u.m.o. in 90-electron $[\text{Os}_6(\text{CO})_{17}\{\text{P}(\text{OMe})_3\}_4]^{2-}$ as being low lying and of a_2' symmetry (3). In terms of bispherical tensor surface harmonics this orbital may be identified as $3\bar{P}_0^\pi$. If this orbital is unoccupied then a 90-electron cluster results [arising from the 48 electrons characteristic of a triangle and 42 electrons (3×14) corresponding to the 14 electrons in metal-carbonyl bonding and metal (d) non-bonding orbitals associated with the outer metal atoms]. Occupation of $3\bar{P}_0^\pi$ leads to a 92-electron cluster based on a 50-electron triangular unit. This situation is clearly analogous to the tricapped trigonal prism where an analogous $3\bar{P}_0^\pi$ orbital is occupied. Such a cluster has been prepared by the reduction of a 90-electron cluster.²³ A related cluster is the platinum-iron complex $[\text{Fe}_3\text{Pt}_3(\text{CO})_{15}]^{2-}$ (4) which has 86 cluster valence electrons²⁴ consisting of 44 electrons for the (inner) $\text{Pt}_3(\text{CO})_3$ triangle and 42 electrons [14 from each $\text{Fe}(\text{CO})_4$ unit] for the outer ring. The characteristic electron count for a Pt_3L_3 triangle is 42 so this cluster has an additional pair of electrons which again reside in the $3\bar{P}_0^\pi$ orbital.²² The recently reported raft cluster $[\text{Cu}_3\text{Fe}_3(\text{CO})_{12}]^{3-}$, which has $\text{Fe}(\text{CO})_4$ groups bridging a Cu_3 triangle,²⁵ only possesses 84 cluster valence electrons. This may be explained in terms of the $3\bar{P}_0^\pi$ orbital being inaccessible for Cu because it possesses more p^π atomic orbital character than in the platinum case, where the terminal CO ligand induces $d^\pi-p^\pi$ mixing. Extended raft clusters are known which either have metal atoms lying on more than two concentric rings or a central metal atom. Examples of such clusters are $[\{\text{Os}_3(\text{CO})_{11}\text{Hg}\}_3]^{2-}$ and $[\text{Cu}_5\text{Fe}_4(\text{CO})_{16}]^{3-}$ (5). The bonding in these clusters can be analysed by an extension of the principles developed above.

Conclusions

The L^σ , L^π , and \bar{L}^π skeletal molecular orbitals of bispherical clusters have been derived from those of the constituent spherical polyhedra. The addition of successive spherical shells leads to skeletal molecular orbitals with radial as well as angular nodes. On deforming bispherical clusters into a spherical topology these radial nodes are converted into additional angular nodes.

Table 4. Examples of bispherical clusters (capped structures)*

Description	Example	Ref.	N_i	N_o	N_t	s.e.p.	Extra s.e.p.
Octahedron	$[\text{Os}_6(\text{CO})_{18}]^{2-}$	<i>a</i>	6	0	6	$7(N_i + 1)$	—
Capped octahedron	$[\text{Os}_7(\text{CO})_{21}]$	<i>b</i>	6	1	7	$7(N_i + 1 = N_t)$	0
Bicapped octahedron	$[\text{Os}_8(\text{CO})_{22}]^{2-}$	<i>c</i>	6	2	8	$7(N_i + 1)$	0
Tetracapped octahedron	$[\text{Os}_{10}\text{C}(\text{CO})_{24}]^{2-}$	<i>d</i>	6	4	10	$7(N_i + 1)$	0
Hexacapped octahedron	$[\text{Pd}_{10}(\text{CO})_{12}(\text{PBu}_3)_6]$	<i>e</i>	6	4	10	$8(N_i + 2)$	1
	$[\text{Pd}_6\text{Fe}_6(\text{CO})_{23}\text{H}]^{3-}$	20	6	6	12	$8(N_i + 2)$	1
Octahedron†	$[\text{Cu}_6(\text{PPh}_3)_6\text{H}_6]$	<i>f</i>	6	0	6	$6(N_i)$	—
Tetracapped octahedron	$[\text{Cu}_6\text{Fe}_4(\text{CO})_{16}]^{2-}$	<i>g</i> , 25	6	4	10	$6(N_i)$	0
	$[\text{Hg}_6\text{Rh}_4(\text{PMe}_3)_{12}]$	<i>h</i>	6	4	10	$6(N_i)$	0
Cube	$[\text{Ni}_8(\text{PPh})_6(\text{CO})_8]$	<i>i</i>	8	0	8	$12(3N_i/2)$	—
Pentacapped cube	$[\text{Rh}_{14}(\text{CO})_{25}]^{4-}$	<i>j</i>	8	5	13	$12(3N_i/2)$	0
(centred)	$[\text{Rh}_{14}(\text{CO})_{26}]^{2-}$	<i>k</i>	8	5	13	$12(3N_i/2)$	0
Rhombic dodecahedron/ hexacapped cube (centred)	$[\text{Rh}_{15}(\text{CO})_{30}]^{3-}$	17	8	6	14	$15[(3N_i/2) + 3 = N_i + 1]$	3
Pentagonal prism	$\text{C}_{10}\text{H}_{10}$	<i>l</i>	10	0	10	$15(3N_i/2)$	—
Tetracapped pentagonal prism (centred)	$[\text{Rh}_{15}\text{C}_2(\text{CO})_{28}]^-$	<i>m</i>	10	4	14	$16[(3N_i/2) + 1]$	1
($2\circ + 2\square$)‡							
Square antiprism§	$[\text{Co}_8\text{C}(\text{CO})_{18}]^{2-}$	<i>n</i>	8	0	8	$9(N_i + 1)$ (<i>closo</i>)	—
Tetracapped square antiprism (4A)	$[\text{Co}_3\text{Ni}_9\text{C}(\text{CO})_{20}]^{3-}$	<i>o</i>	8	4	12	$10(N_i + 2)$	1

Table 4 (continued)

Description	Example	Ref.	N_i	N_o	N_t	s.e.p.	Extra s.e.p.
Square antiprism	$[\text{Ni}_8\text{C}(\text{CO})_{16}]^{2-}$ $[\text{Bi}_8]^{2+}$	<i>o</i>	8	0	8	11 ($N_i + 3$) (<i>arachno</i>)	—
		<i>p</i>	8	0	8	11 ($N_i + 3$) (<i>arachno</i>)	—
Trigonal prism	C_6H_6 $[\text{Rh}_6\text{C}(\text{CO})_{15}]^{2-}$	<i>q</i> <i>r</i>	6	0	6	9 ($3N_i/2$)	—
Capped (and edge-bridged) trigonal prism (1□)	$[\text{Rh}_8\text{C}(\text{CO})_{19}]$	<i>s</i>	6	1	7	9 ($3N_i/2$)	0
Bicapped trigonal prism (2△)	$[\text{Cu}_2\text{Rh}_6\text{C}(\text{CO})_{15}(\text{NCMe})_2]$	<i>t</i>	6	2	8	9 ($3N_i/2$)	0
Tricapped trigonal prism (3□)	$[\text{B}_9\text{H}_9]^{2-}$ $[\text{TiSn}_8]^{3-}$ $[\text{Bi}_9]^{5+}$ †	<i>u</i>	6	3	9	10 [$(3N_i/2) + 1 = N_i + 1$]	1
		<i>v</i>				11 [$(3N_i/2) + 2 = N_i + 2$]	2
		<i>w</i>					
Square-face-sharing fused trigonal prisms (A)	$[\text{Co}_6\text{Ni}_2\text{C}_2(\text{CO})_{16}]^{2-}$	<i>x</i>	8	0	8	10	—
Bicapped A (2□)	$[\text{Ni}_{10}\text{C}_2(\text{CO})_{16}]^{2-}$	<i>y</i>	8	2	10	11	1
Twinned cuboctahedron (centred)	$[\text{Rh}_{13}(\text{CO})_{24}\text{H}_{5-n}]^{n-}$	<i>z</i>	12	0	12	13 ($N_i + 1$)	—
Cuboctahedron			12	0	12	13 ($N_i + 1$)	—
Distorted tetracapped cuboctahedron (4□)	$[\text{Ni}_{16}\text{C}_4(\text{CO})_{23}]^{4-}$	<i>aa</i>	12	4	16	17 ($N_i + 5 = N_i + 1$)	4
Hexacapped (and edge-bridged) cuboctahedron (centred) (6□)	$[\text{Pd}_{23}(\text{CO})_{22}(\text{PEt}_3)_{10}]$	<i>bb</i>	12	6	18	15 ($N_i + 3$)	2

* N_i = Number of inner-sphere atoms (central core); N_o = number of outer-sphere (capping) atoms (not counting edge-bridging groups which form essentially localised two-centre two-electron bonds to the inner-sphere polyhedron); N_t = total number of cluster atoms (not counting central/interstitial atoms or edge-bridging atoms, which donate all their valence electrons to the cluster).

† Polyhedral clusters of the Group 1B and 2B metals generally have one skeletal electron pair less than normal. Octahedral clusters of this type are therefore characterised by 84 cluster valence electrons. Another example of a bispherical cluster based on an 84-electron octahedron is $[\text{Ag}_6\{\text{Fe}(\text{CO})_4\}_3\{\text{Ph}_2\text{P}\}_3\text{CH}]$ which has three faces capped by $\text{Fe}(\text{CO})_4$ groups and the other capped by a tripodal phosphine ligand (C. E. Briant, R. G. Smith, and D. M. P. Mingos, *J. Chem. Soc., Chem. Commun.*, 1984, 586). ‡ The numbers in brackets refer to the number and type of face which is capped, in those cases where the inner-sphere polyhedron possesses more than one type of face. § The square antiprism may be regarded as either a four-connected polyhedron (in which case it should possess $N + 1 = 9$ s.e.p.s as for a *closo* cluster) or an *arachno* deltahedron (characterised by $N + 3 = 11$ s.e.p.s).⁷ ¶ For the $[\text{Bi}_9]^{5+}$ cluster both $3P_0^*$ and $3P_0^*$ are occupied ($3P_0^*$ is a fairly low-lying l.u.m.o. for $[\text{B}_9\text{H}_9]^{2-}$); refs. 6, 14, and K. Wade and M. E. O'Neill, *Polyhedron*, 1983, 2, 963. ^a M. McPartlin, C. R. Eady, B. F. G. Johnson, and J. Lewis, *J. Chem. Soc., Chem. Commun.*, 1976, 883. ^b C. R. Eady, B. F. G. Johnson, J. Lewis, R. Mason, P. B. Hitchcock, and K. M. Thomas, *J. Chem. Soc., Chem. Commun.*, 1977, 385. ^c P. F. Jackson, B. F. G. Johnson, J. Lewis, and P. R. Raithby, *J. Chem. Soc., Chem. Commun.*, 1980, 60. ^d P. F. Jackson, B. F. G. Johnson, J. Lewis, W. J. H. Nelson, and M. McPartlin, *J. Chem. Soc., Dalton Trans.*, 1982, 2099. ^e E. G. Mednikov, N. K. Eremenko, S. P. Gubin, Yu. L. Slovokhotov, and Yu. T. Struchkov, *J. Organomet. Chem.*, 1982, 239, 401. ^f M. R. Churchill, S. A. Bezman, J. A. Osborn, and J. Wormald, *Inorg. Chem.*, 1972, 11, 1818. ^g G. Doyle, B. T. Heaton, and E. Ochiello, *Organometallics*, 1985, 4, 1224. ^h R. A. Jones, F. M. Real, G. Wilkinson, A. M. R. Galas, and M. B. Hursthouse, *J. Chem. Soc., Dalton Trans.*, 1981, 126. ⁱ L. D. Lower and L. F. Dahl, *J. Am. Chem. Soc.*, 1976, 98, 5046. ^j G. Ciani, A. Sironi, and S. Martinengo, *J. Organomet. Chem.*, 1980, 192, C42. ^k S. Martinengo, G. Ciani, and A. Sironi, *J. Chem. Soc., Chem. Commun.*, 1980, 1140. ^l P. E. Eaton, Y. S. Or, and S. J. Branca, *J. Am. Chem. Soc.*, 1981, 103, 2134. ^m V. G. Albano, M. Sansoni, P. Chini, S. Martinengo, and D. Strumulo, *J. Chem. Soc., Dalton Trans.*, 1976, 970. ⁿ V. G. Albano, P. Chini, G. Ciani, S. Martinengo, and M. Sansoni, *J. Chem. Soc., Dalton Trans.*, 1978, 463. ^o G. Longoni, A. Ceriotti, R. Della Pergola, M. Manassero, M. Perego, G. Piro, and M. Sansoni, *Philos. Trans. R. Soc. London, A*, 1982, 308, 47. ^p J. D. Corbett, *Inorg. Chem.*, 1968, 7, 198; B. Krebs, M. Hücke, and C. J. Brendel, *Angew. Chem., Int. Ed. Engl.*, 1982, 21, 445. ^q T. J. Katz and N. Acton, *J. Am. Chem. Soc.*, 1973, 95, 2738. ^r V. G. Albano, D. Braga, and S. Martinengo, *J. Chem. Soc., Dalton Trans.*, 1981, 717. ^s P. R. Raithby, in 'Transition Metal Clusters,' ed. B. F. G. Johnson, Wiley, New York, 1980, ch. 2, p. 63. ^t V. G. Albano, D. Braga, S. Martinengo, P. Chini, M. Sansoni, and D. Strumulo, *J. Chem. Soc., Dalton Trans.*, 1980, 52. ^u F. Klanberg and E. L. Muetterties, *Inorg. Chem.*, 1966, 5, 1955. ^v R. C. Burns and J. D. Corbett, *J. Am. Chem. Soc.*, 1982, 104, 2804. ^w A. Herschaft and J. D. Corbett, *Inorg. Chem.*, 1963, 2, 979; R. M. Friedman and J. D. Corbett, *Inorg. Chim. Acta*, 1973, 7, 525. ^x A. Arrigoni, A. Ceriotti, R. Della Pergola, G. Longoni, M. Manassero, N. Masciocchi, and M. Sansoni, *Angew. Chem., Int. Ed. Engl.*, 1984, 23, 322. ^y A. Ceriotti, G. Longoni, M. Manassero, N. Masciocchi, L. Resconi, and M. Sansoni, *J. Chem. Soc., Chem. Commun.*, 1985, 181. ^z G. Ciani, A. Sironi, and S. Martinengo, *J. Chem. Soc., Dalton Trans.*, 1981, 519. ^{aa} A. Ceriotti, G. Longoni, M. Manassero, N. Masciocchi, G. Piro, L. Resconi, and M. Sansoni, *J. Chem. Soc., Chem. Commun.*, 1985, 1402. ^{bb} E. G. Mednikov, N. K. Eremenko, Yu. L. Slovokhotov, and Yu. T. Struchkov, *J. Organomet. Chem.*, 1986, 301, C35.

In the bispherical extremes the clusters are characterised by a skeletal electron-pair count corresponding to the occupation of the bonding molecular orbitals of the inner polyhedron and certain \bar{L}^n orbitals (predominantly localised on the outer sphere) which are lowered due to a bonding interaction between the molecular orbitals of the two polyhedra. The number of additional skeletal bonding molecular orbitals depends upon the topology of the atoms lying on the outer sphere and the mismatch in symmetry between the L^n molecular orbitals of the inner-sphere polyhedron and the \bar{L}^n molecular orbitals of the

outer-sphere polyhedron. In the case where the outer-sphere polyhedral topology is spherical, three additional orbitals are generally stabilised. These orbitals are \bar{P}^n if the central polyhedron is three-connected and \bar{D}^n , \bar{F}^n , etc. if it is a deltahedron. If, however, the topology of the outer-sphere atoms is toroidal (planar or puckered rings) only one component of these orbitals is lowered. These concepts have also been applied to the study of planar raft clusters where again only one additional orbital (\bar{P}_0^*) is stabilised.

A rhombohedral 'spherical' cluster lies at the midpoint

between the two (omnicapped) bispherical extremes. This cluster is characterised by $(N + 1)$ skeletal electron pairs and its molecular orbitals may be correlated with those of the bispherical clusters.

Acknowledgements

The S.E.R.C. is thanked for financial support.

References

- 1 A. J. Stone, *Mol. Phys.*, 1980, **41**, 1339.
- 2 A. J. Stone, *Inorg. Chem.*, 1981, **20**, 563.
- 3 A. J. Stone and M. J. Alderton, *Inorg. Chem.*, 1982, **21**, 2297.
- 4 A. J. Stone, *Polyhedron*, 1984, **3**, 2051.
- 5 K. Wade, *Chem. Commun.*, 1971, 792; *Inorg. Nucl. Chem. Lett.*, 1972, **8**, 559, 563; *Adv. Inorg. Chem. Radiochem.*, 1976, **18**, 1; D. M. P. Mingos, *Nature, Phys. Sci. (London)*, 1972, **236**, 99; R. Mason, K. M. Thomas, and D. M. P. Mingos, *J. Am. Chem. Soc.*, 1973, **95**, 3802.
- 6 R. L. Johnston and D. M. P. Mingos, *J. Organomet. Chem.*, 1985, **280**, 407.
- 7 R. L. Johnston and D. M. P. Mingos, *J. Organomet. Chem.*, 1985, **280**, 419.
- 8 A. Ceulemans, *Mol. Phys.*, 1985, **54**, 161.
- 9 D. B. Redmond, C. M. Quinn, and J. G. R. McKiernan, *J. Chem. Soc., Faraday Trans. 2*, 1983, 1791.
- 10 P. W. Fowler, *Polyhedron*, 1985, **4**, 2051.
- 11 R. L. Johnston and D. M. P. Mingos, *Polyhedron*, 1986, **5**, 2059.
- 12 See, for example, B. E. Douglas and C. A. Hollingsworth, 'Symmetry in Bonding and Spectra (An Introduction),' Academic Press, New York, 1985, ch. 7.3, p. 193.
- 13 P. Brint, J. P. Cronin, and E. Seward, *J. Chem. Soc., Dalton Trans.*, 1983, 675.
- 14 R. L. Johnston and D. M. P. Mingos, *J. Chem. Soc., Dalton Trans.*, 1987, 647.
- 15 H. M. Cundy and A. P. Rollett, 'Mathematical Models,' 3rd edn., Tarquin, Stradbroke, Norfolk, 1981.
- 16 M. I. Forsyth and D. M. P. Mingos, *J. Chem. Soc., Dalton Trans.*, 1977, 610.
- 17 J. L. Vidal, L. A. Kopicak, and J. M. Troup, *J. Organomet. Chem.*, 1981, **215**, C11.
- 18 D. M. P. Mingos, *J. Chem. Soc., Chem. Commun.*, 1985, 1352; *Chem. Soc. Rev.*, 1986, **15**, 31.
- 19 R. L. Johnston and D. M. P. Mingos, unpublished work.
- 20 G. Longoni, M. Manasserro, and M. Sansoni, *J. Am. Chem. Soc.*, 1980, **102**, 3242.
- 21 R. J. Goudsmit, B. F. G. Johnson, J. Lewis, P. R. Raithby, and K. H. Whitmire, *J. Chem. Soc., Chem. Commun.*, 1982, 640.
- 22 D. G. Evans and D. M. P. Mingos, *Organometallics*, 1983, **2**, 435.
- 23 J. G. Jeffrey, Ph.D. Thesis, Cambridge University, 1985.
- 24 G. Longoni, M. Manasserro, and M. Sansoni, *J. Am. Chem. Soc.*, 1980, **102**, 7973.
- 25 G. Doyle, K. A. Eriksen, and D. Van Engen, *J. Am. Chem. Soc.*, 1986, **108**, 445.
- 26 M. Fajardo, H. D. Holden, B. F. G. Johnson, J. Lewis, and P. R. Raithby, *J. Chem. Soc., Chem. Commun.*, 1984, 24.

Received 7th July 1986; Paper 6/1348